A HAFNIUM-FREE DIRECTIONALLY SOLIDIFIED

NICKEL-BASE SUPERALLOY

Dongliang Lin (T. L. Lin) and Songhui Huang
Department of Materials Science and Engineering
Shanghai JIao Tong University, Shanghai, China

Chuanqi Sun
Institute of Aeronautic Materials
Beijing, China

Abstract

This paper provides a review of current efforts on design of a hafnium-free directionally solidified nickel-base superalloy with good castability, post-casting transverse ductility and improved creep strength in our laboratories. Emphasis is being placed on the effect of alloy modifications on castability and the improvement of creep strength by increasing solid solution temperature.

Introduction

Although the benefits of directionally solidified (DS) alloys have been amply realized, there is still much room for improvement. Hafnium was added to DS MAR-M200 to prevent grain boundary cracking of hollow-blade castings during solidification and to provide good post-casting transverse ductility (1,2,3). However, the addition of hafnium had led to the formation of hafnium containing inclusions which affected casting yields and lowered the incipient melting temperature, which in turn limited possible increases in solution temperature for further strengthening DS nickel-base superalloys by improving their creep strength. In order to overcome the shortcomings of hafnium containing DS superalloys, hafnium should be minimized or eliminated and, perhaps, replaced with other grain boundary strengthening elements, and a hafnium-free superalloy with good castability and post-casting transverse ductility developed.

In recent years, a DS nickel-base superalloy, DZ-3 has been developed in our laboratories based on a cast nickel-base superalloy, K3. This alloy was developed in our laboratories in the early 1960's and has been widely used since then in China for first and second turbine blades and vanes in various kinds of aircraft engines (4). As a DS alloy, the composition of DZ-3 was modified from that of alloy K3 as shown in Table 1. It has been shown that the advantages of directionally solidified superalloy, DZ-3 over conventional cast superalloy, K3 are better creep properties, greater thermal fatigue life, greater rupture life, and greater rupture ductility, which are comparable to those of DS alloy PWA 1422 (5). However, in many instances, cracking of hollow airfoils is associated with thin walls present in the castings of DZ-3. By proper positioning of the core in the mold and close matching of the core and wax tooling, this difficulty can be partly overcome. The addition of hafnium to DZ-3 alloy can also reduce the tendency for grain boundary cracking. In order to completely prevent grain-boundary

Superalloys 1988
Edited by S. Reichman, D.N. Duhl,
G. Maurer, S. Antolovich and C. Lund
The Metallurgical Society, 1988

cracking of hollow blade casting during directional solidification and to provide good post-casting transverse ductility, an alloy modification of DZ-3 has been investigated and results compared with the effects of hafnium additions. A new hafnium-free DS alloy called DZ-4 was developed and its composition is listed in Table 1. A large number of DS hollow-airfoils have been successfully cast with DZ-4 alloy (Fig. 1).

This paper provides a review of the alloy design with emphasis placed on the effect of alloy modifications on castability and the improvement of creep strength by increasing the solution temperature.

Table 1. Composition of K3, DZ-3, and DZ-4

	C	Cr	Co	W	Mo	Al	Ti	Ti+Al	B	Ce	Zr	Ni
K3	0.11	10.0	4.5	4.8	3.8	5.3	2.3		0.01	0.01	0.1	Bal
	0.18	12.0	6.0	5.5	4.5	5.9	2.9		0.03	0.03		
DZ-3	0.07	9.5	4.5	4.8	3.8	5.2	2.3		0.015	0.01	0.1	Bal
	0.15	11.0	6.0	5.8	4.6	5.9	2.9		0.03			
DZ-4	0.10	9.0	5.5	5.1	3.5	5.6	1.6	>7.6	0.012			Bal
	0.16	10.0	6.0	5.8	4.2	6.4	2.2		0.025			

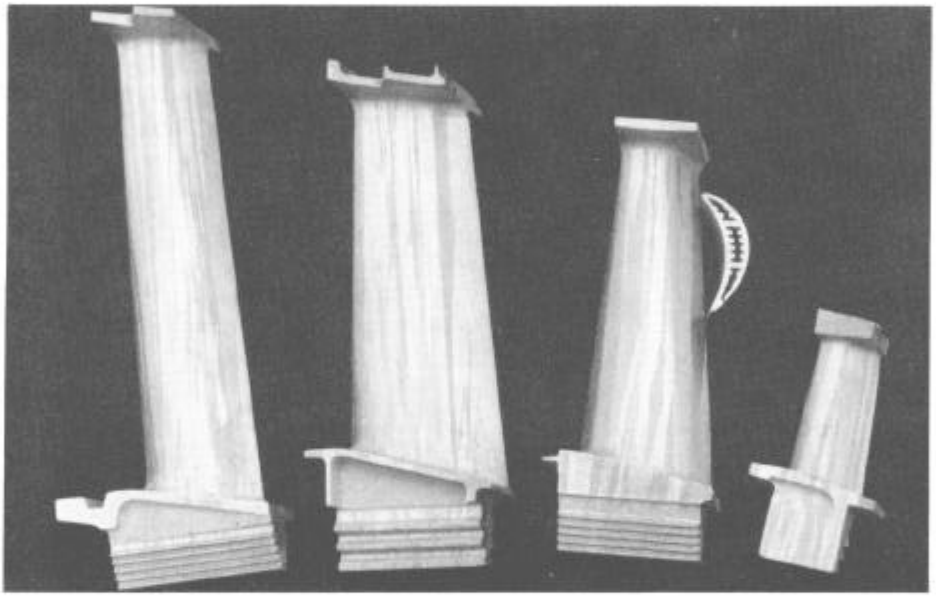

Fig. 1 Hollow airfoils directionally solidified in DZ-4.

Castability Improvement by Alloy Modification

It has been shown that Zr and Ti are the elements which tend to enlarge the melting and solidification range of alloys, $\Delta T=T_L-T_S$, where T_L, T_S are the liquidus and solidus temperatures of an alloy.

The composition of the experimental alloys studied to assess castability are shown in Table 2. Alloy 1 is DZ-3, the baseline alloy. In alloys 2 to 4, Zr is eliminated and 0.3 to 0.8 weight percent (w/o) Ti is replaced by 0.6 to 0.9 w/o Al. In alloys 6 to 10, various amounts of hafnium from 0.3 to 2.0 w/o are added to DZ-3. The cracking tendency on both inner and outer surfaces of the hollow-blade castings was selected as a measure of alloy castability. A typical crack on the surface of a DZ-3 hollow-blade is shown in Fig. 2. Five sections (I, II, III, IV, and V) of a hollow-blade with a minimum of 0.8 mm and a maximum of 3.3 mm in thickness were chosen as the location to examine for the presence of cracks using penetrant inspection and optical microscopy. The degree of castability was divided into four

classes: A - no cracks; B - no more than 2 cracks with a length of less than 5 mm in any of the sections; C - no cracks on the outer surface of all five sections, but cracks on the inner surfaces; and D - cracks on inner and outer surfaces of all five sections.

The results of the castability tests listed in Table 3 indicate that the Zr-free alloys 2, 4 and 5 where some of the Ti has been replaced by Al and alloy 10 with 2% Hf display superior castability compared to the other

Table 2. Chemical Composition of Experimental Alloys, Weight Percent

Alloy No.	C	Cr	Co	W	Mo	Al	Ti	B	Ce	Zr	Hf	Ni
1	0.14	10	5.0	5.4	4.3	5.4	2.6	0.015	0.01	0.1		Bal
2	0.14	10	6.0	5.9	3.8	6.0	1.8	0.015				Bal
3	0.14	10	5.0	5.4	4.3	5.4	2.5	0.015				Bal
4	0.17	10	6.0	5.9	3.8	6.3	2.3	0.015				Bal
5	0.10	9	5.0	5.4	3.8	5.3	1.6	0.015				Bal
6	0.14	10	5.0	5.4	4.3	5.4	2.6	0.015	0.01	0.1	0.3	Bal
7	0.14	10	5.0	5.4	4.3	5.4	2.6	0.015	0.01	0.1	0.6	Bal
8	0.14	10	5.0	5.4	4.3	5.4	2.6	0.015	0.01	0.1	1.0	Bal
9	0.14	10	5.0	5.4	4.3	5.4	2.6	0.015	0.01	0.1	1.5	Bal
10	0.14	10	5.0	5.4	4.3	5.4	2.6	0.015	0.01	0.1	2.0	Bal

Table 3. Castability of Experimental Alloys

Alloy No.	Solidification Process	Volume Percent	Castability Rank	Yield (A Rank)
1	DS	57.9	D	0
2	DS	57.4	A	100
3	DS	57.9	C	50
4	DS	63.4	A	100
5	DS	52.8	A	100
6	DS	57.8	B	25
7	DS	58.1	B	40
8	DS	58.6	B	60
9	DS	59.5	B	75
10	DS	60.37	A	100
2	CC	57.9	A	100

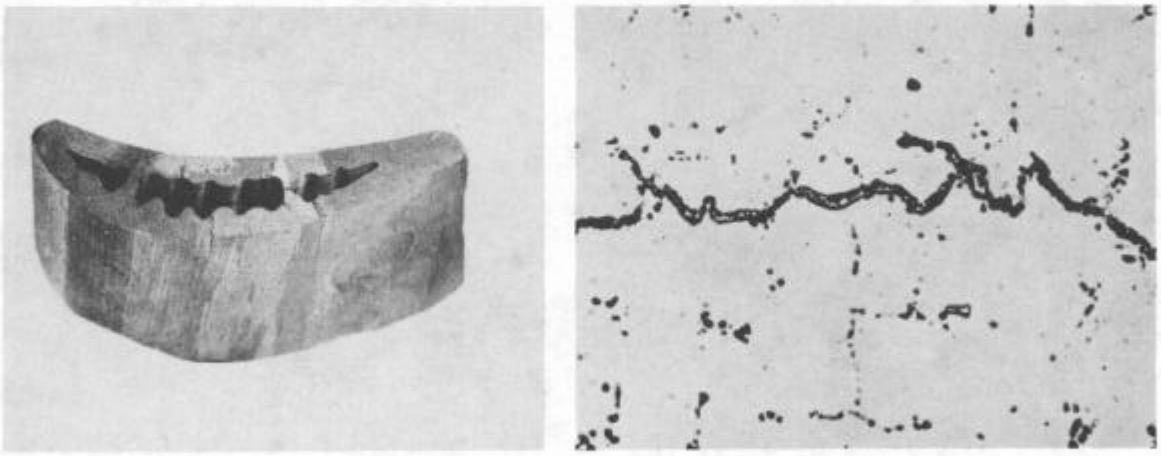

(a) (b)

Fig. 2 A typical crack in a hollow blade of alloy DZ-3 (a) and its micrograph at higher magnification (b).

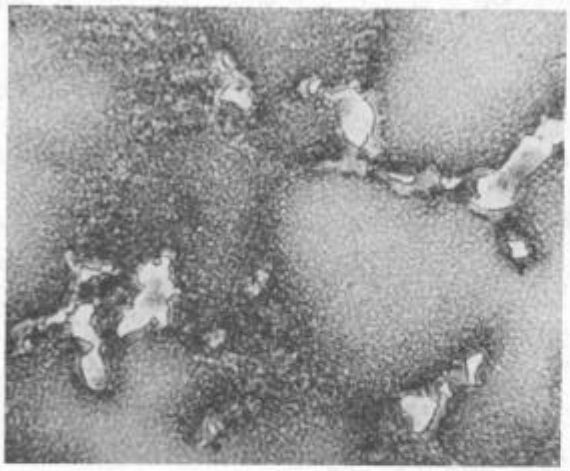

(a) As-cast state, alloy 1

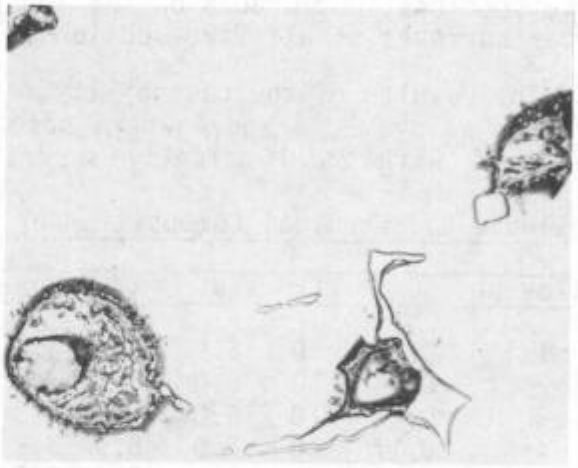

(b) Quenched from 1250°C/1h, alloy 1

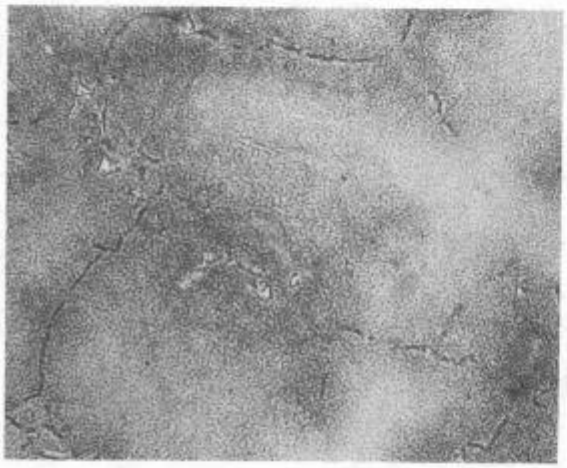

(c) As-cast state, alloy 2

(d) Quenched from 1290°C/1h, alloy 2

(e) As-cast state, alloy 10

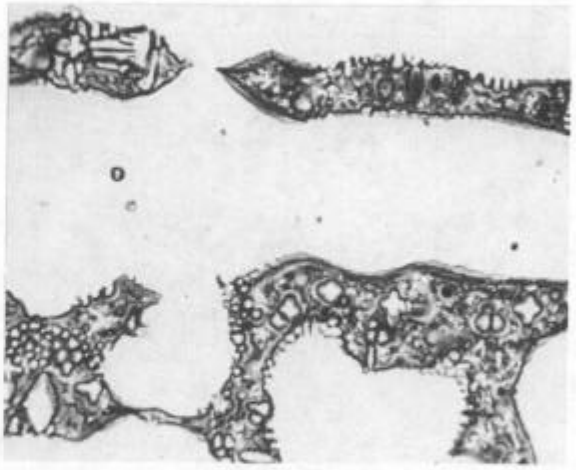

(f) Quenched from 1290°C/1h, alloy 10

Fig. 3 Microstructure of the experimental alloys.

alloys. The differential thermal analysis and quenching method were used to determine the melting and solidification range of the alloys and some results are shown in Table 4. Both liquidus and solidus temperatures of alloy 2 (DZ-4) are higher than those of alloy 1 (DZ-3) especially during cooling where the solidus temperature of alloy 2 is 30°C higher than that of alloy 1. The solidus temperature for alloy 10 (DZ-3 with 2% Hf) is 26°C lower than that of alloy 1 and 56°C lower than that of alloy 2. Since there is no $\gamma+\gamma'$ eutectic in alloy 2, as shown in Fig. 3c, its incipient melting temperature is greater than 1290°C, while alloy 1 starts to incipiently melt at 1170°C (Fig. 3b and 4) because it contains 2.0 to 4.7 volume percent of $\gamma+\gamma'$ eutectic (Fig. 3a). This suggests that grain-boundary cracking of hollow-blade castings can be prevented by the elimination of $\gamma+\gamma'$ eutectic (6). However, in hafnium containing alloys, the $\gamma+\gamma'$ eutectic increases as the Hf content increases. When an alloy contains greater than 1.5 w/o Hf, the amount of the $\gamma+\gamma'$ eutectic is 24 volume percent as in the case of alloy 10 (Fig. 3e) which contains 2 w/o Hf. Therefore, grain boundary cracking can be avoided by producing a large amount of $\gamma+\gamma'$ eutectic in DS superalloys. In summary, an improved understanding of the solidification process, the local chemistry and microstructure that control grain boundary strength would be useful to explain these phenomena. A hafnium-free DS superalloy, DZ-4, was developed to meet the requirements for hollow-blade castings based on the compositions of alloys 2 and 4.

Table 4. Differential Thermal Analysis

Alloy No.	Heating			Cooling		
	Liquidus Temperature	Solidus Temperature	Melting Range	Liquidus Temperature	Solidus Temperature	Melting Range
1	1356°C	1296°C	60°C	1347°C	1266°C	81°C
2	1365	1309	56	1356	1296	60
10	1339	1260	79	1335	1240	95

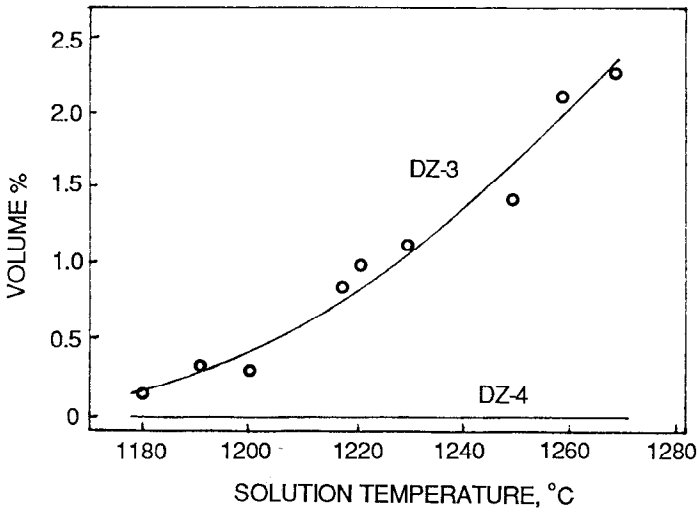

Fig. 4 Amount of incipient melting phase as a function of solution temperature for DZ-3 and DZ-4.

Creep Strength and Rupture Life Improvement by Increasing Solid Solution Temperature

It has been shown that solution treatments at temperatures sufficiently high to homogenize the alloy and dissolve the coarse γ' and eutectic $\gamma+\gamma'$ constituent for reprecipitation in the form of a uniform fine γ' dispersion will further strengthen DS nickel-base alloys by improving their creep strength. J. J. Jackson and his co-workers (7) found a threefold increase in creep rupture life at 982°C under 220 MPa in DS MAR-M200 + Hf when the

amount of fine γ' increased from about 30 volume percent to approximately 45 volume percent. The role of high temperature solution treatments in increasing the creep strength and rupture life of DS nickel-base superalloys has been investigated systematically by Dongliang Lin (T. L. Lin) and his co-workers (8,9) and it was found that the secondary creep rate at 760°C is related to the size a, center departure L or particle spacing λ and volume fraction V_f of fine γ' particles as follows:

$$\varepsilon \alpha \lambda^2/a \text{ or } \varepsilon \alpha a/V_f^{2/3}\left(1-V_f^{2/3}\right)^2 \text{ for alloy DZ-3}$$

and $$\varepsilon \alpha L^2/a \text{ or } \varepsilon \alpha a/V_f^{2/3} \text{ for alloy DZ-17G and DS René 80}$$

The smaller the size and the higher the volume fraction of fine γ', the lower the secondary creep rate. The relation between rupture life t_f and secondary creep rate ε was found to fit the following expression:

$$t_f \varepsilon^{\alpha} = C\varepsilon_f$$

where α and C are alloy constants. The extension of creep rupture life was found to be due to a decrease of the secondary creep rate and an extension of the secondary creep stage. Raising the solution temperature will increase the volume fraction and decrease the size of the fine γ' which leads to a lower secondary creep rate and extends rupture life. The limitation for increasing the solution temperature is the low incipient melting temperature for alloys containing $\gamma+\gamma'$ eutectic. As mentioned above, DZ-4 has its incipient melting point greater than 1290°C (Fig. 3b and 4), so it is possible to further increase its creep strength and extend its rupture life by increasing its solution temperature. Fig. 5 and 6 show that either rupture life or tensile strength at 760°C and 980°C for DZ-4 can be significantly improved by increasing the solution temperature to 1270°C.

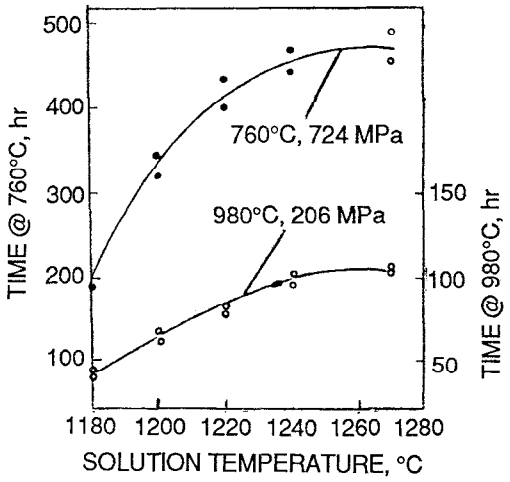

Fig. 5 Solution temperature vs. rupture life for alloy DZ-4.

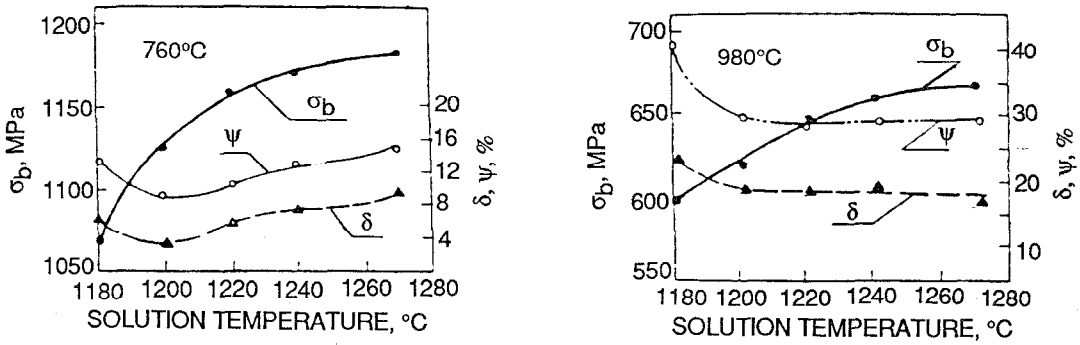

Fig. 6 Solution temperature vs. tensile properties at 760°C and 980°C for DZ-4.

The size, a, and volume fraction, V_f, of fine cuboidal γ' were determined by area measurements on representative electron photomicrographs and then the separation of γ' particles was calculated by the method described in Ref. 5.

Specimens of DZ-4 were solution treated at 1180, 1200, 1220, 1240, and 1270°C for 2 h/AC. All specimens for creep rupture testing were aged for 16 hours at 870°C after the solution treatment. The morphology and size of γ' in solution treated DZ-4 are shown in Fig. 7. The as-cast coarse γ' was dissolved gradually with increasing solution temperature and fine cuboidal γ' was reprecipitated during subsequent cooling, while undissolved γ' coalesced. At 1220°C, the as-cast coarse γ' was completely dissolved in the dendritic regions and only a few retained as-cast γ' particles existed in the interdendritic regions. Above 1230°C, a fine uniform cuboidal γ' could be found after solution treatment. The volume fraction V_f and size a (the side of a cuboid) of fine γ' after solution treatment at various temperatures, followed by aging at 870°C for 16 hours, are shown in Fig. 8. The largest volume fraction V_f and the smallest fine γ' size can be obtained by solutioning above 1270°C, which is the solution temperature to obtain the optimum rupture life and tensile strength at 760°C and 980°C for DZ-4. Therefore, solution temperature can be raised from 1210-1230°C for DZ-3 to 1260-1280°C for DZ-4.

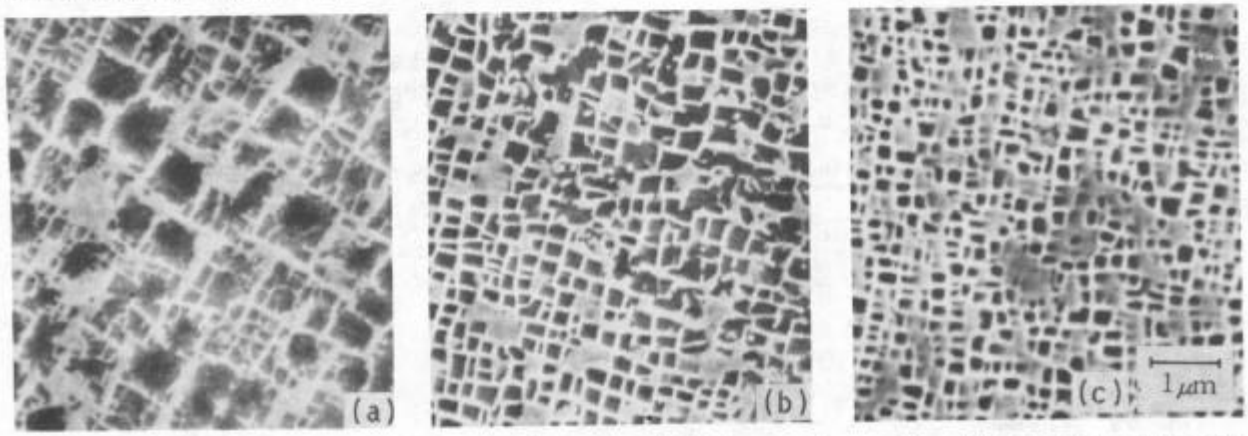

Fig. 7 γ' phase morphology in interdendritic regions for DZ-4 after 1180°C (a), 1220°C (b), and 1290°C (c) solutioning and 870°C/16h aging.

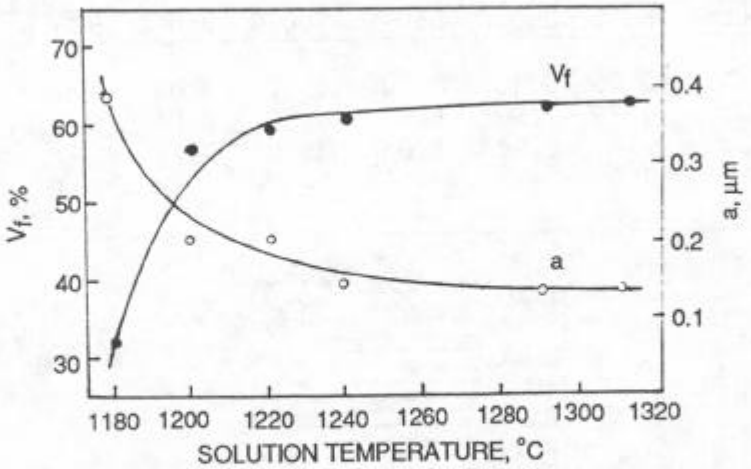

Fig. 8 Solution temperature vs. volume fraction, V_f, and size, a, of fine γ'.

Mechanical Properties of DZ-4

Additional benefits in mechanical properties and phase stability of DZ-4 can be achieved with low values of Nv (Nv = 2.16). The mechanical proper-

ties shown below are for specimens given a standard heat treatment, e.g., 1220°C/4h/AC + 870°C/32h/AC. DZ-4 presently under development has a higher incipient melting temperature (>1290°C). One can therefore increase the solution temperature to provide a more homogenous and uniform distribution of fine γ' which will lead to further increases in alloy strength.

Tensile Strength

As shown in Table 5, the tensile strength and ductility of DZ-4 are comparable with those of advanced DS superalloys.

Table 5. Tensile Properties

	20°C			760°C			980°C		
Alloy	UTS MPa	YS Mpa	EL %	UTS Mpa	YS Mpa	EL %	UTS Mpa	YS MPa	EL %
DZ-4	1059	947	6.0	1187	996	6.0	647	466	20
PWA 1422	1108	941	6.1	1187	961	9.4	608	470	21
DZ-3	971	-	5.0	1167	-	15	666	-	21
K3	912	-	5.1	-	-	-	-	-	-

Stress Rupture Strength

With superior rupture strength (Table 6) and reasonable density (Table 7), DZ-4 displays superiority in specific stress rupture strength and temperature capability over other alloys as shown in Table 7 and Fig. 9.

Table 6. 100-Hour Stress Rupture Strength (MPa)

Alloy	760°C	800°C	850°C	900°C	950°C	980°C	1000°C	1040°C	1090°C
DZ-4	840	677	520	353	245	206	181	142	78.5
DZ-3	755	628	490	343	235	206	177	137	78.5
K3	-	520	392	294	216	171	147	-	-
PWA 1422	755	-	-	-	-	200	-	127	-
Mar-M200	741	-	-	-	-	-	-	118	-

Table 7. Specific Stress Rupture Strength

Alloy	Density	760°C	800°C	850°C	900°C	950°C	980°C	1000°C	1040°C
DZ-4	8.15	10.06	8.46	6.50	4.41	3.06	2.57	2.26	1.77
DZ-3	8.10	9.75	7.90	6.17	4.32	2.96	2.59	2.20	1.72
K3	8.10	-	6.54	5.06	3.70	2.71	-	1.85	-
PWA 1422	8.56	9.00	-	-	-	-	2.38	-	1.52
DS-IN100	7.75	8.77	-	-	-	-	2.26	-	-

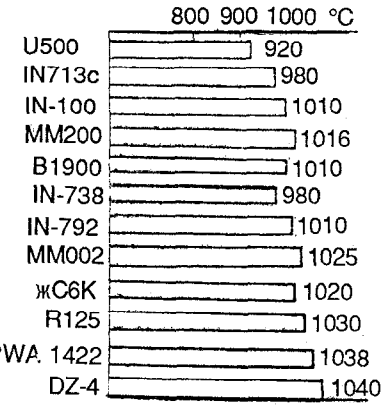

Fig. 9 Temperature capability of alloys at 137 MPa for 100 hours.

Creep Strength

Creep curves at 760°C and 980°C are shown in Fig. 10 and display low secondary creep rates, long rupture life, and high rupture ductility. It should be emphasized that the primary creep strain of DZ-4 at intermediate temperature and high stress is very low, similar to that of DZ-3 (10) and unlike DS MAR-M200 which exhibits relatively large primary creep strains at high stresses and temperatures around 760°C (11).

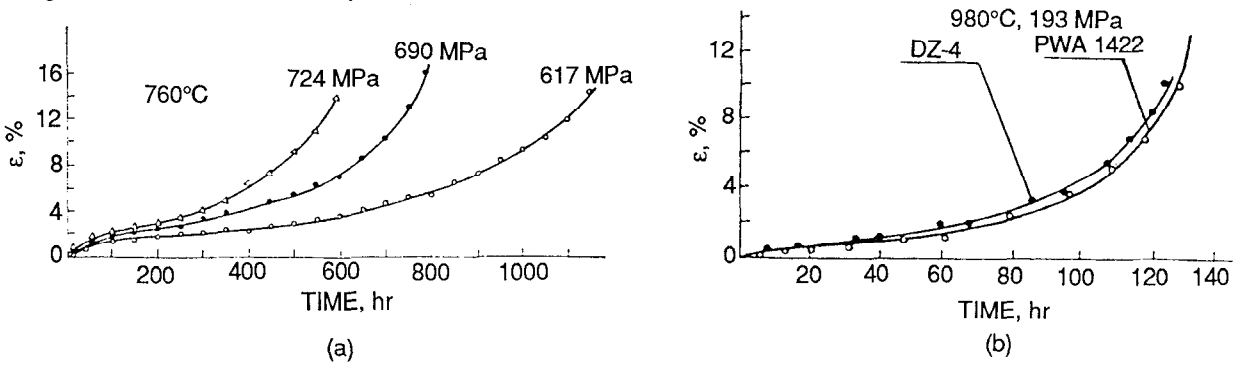

Fig. 10 Creep curves at 760°C for DZ-4 (a) and at 980°C for DZ-4 and PWA 1422 (b).

Thermal Mechanical Fatigue (TMF)

Thermal fatigue cracks in many advanced cooled turbine blades initiate in the coating at the blade leading edge and propagate into the superalloy. Fig. 11 shows the results of a laboratory stress-controlled TMF test that simulates blade cracking. The results for low cycle fatigue (LCF) in Fig. 11 show that the LCF life is greater than that for TMF. If the operating stress for a turbine blade is 196 MPa, its thermal fatigue life will be more than 10,000 cycles.

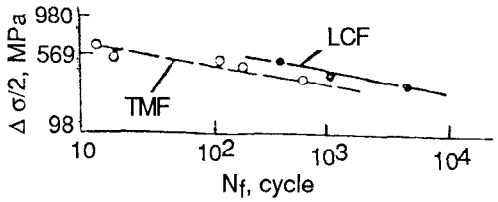

Fig. 11 Curves of LCF and TMF at 980°C.

Transverse Stress Rupture Properties

The results for transverse rupture strength (Table 8) for DZ-4 show that the 100-hour transverse rupture strength is 85% of the longitudinal strength at intermediate temperatures and 90% at higher temperatures. Compared to alloy DZ-3, more Al has been added to DZ-4 replacing some Ti and Zr has been eliminated. DZ-4 has a much longer rupture life and much higher rupture ductility which are the same levels as those of alloys with hafnium, e.g., DS M002 and PWA 1422 (Fig. 12).

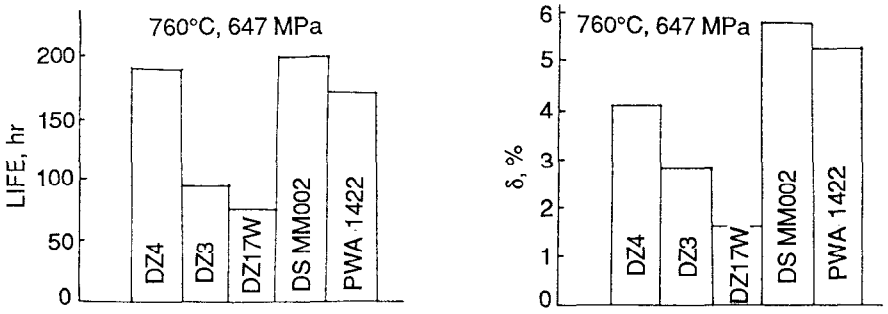

Fig. 12 Transverse rupture life and ductility of various alloys.

Table 8. Transverse Stress Rupture Strength of DZ-4

Orientation	Rupture Strength for 100 hours, MPa 760°C	850°C	980°C	1040°C
Transverse	674	441	181	128
Longitudinal	804	520	206	142
$K = \sigma_T/\sigma_L$	0.84	0.85	0.87	0.90

Conclusions

1. Alloy DZ-4 has been developed to meet the requirements for preventing grain-boundary cracking of hollow-blade castings during directional solidification. It is a hafnium-free DS nickel-base superalloy with good castability and superior high temperature mechanical properties for application as hollow turbine blades and vanes.

2. An alloy modification of DZ-3, made by eliminating Zr and replacing a certain amount of Ti with Al, can significantly improve alloy castability due to reduction in the solidification range ΔT and elimination of the formation of $\gamma+\gamma'$ eutectic. This leads to the prevention of grain-boundary cracking in hollow-blade castings.

3. DZ-4 has a higher incipient melting temperature (>1229°C) which permits an increase in solution temperature and provides an increase in rupture strength and tensile strength with increasing solution temperature up to 1270°C.

References

1. D. N. Duhl and C. P. Sullivan, "Some Effects of Hafnium Additions on the Mechanical Properties of a Columnar-Grained Nickel-Base Superalloy," J. Metals, 23(7)(1971), 38-40.
2. B. H. Kear et al., "Transverse Grain Boundary Strengthening in a DS Nickel-Base Alloy," (Paper presented at the International Conference on the Strength of Metals and Alloys, Cambridge, Aug. 1973), 134-138.
3. Wang Yuping et al., "Influence of Hf Content on Microstructure and Mechanical Properties of DS Superalloy DZ 22," (Proceedings on Cast Superalloy, China, 1986), 47-52.
4. Yin Keqing and Li Qijuan, "Test of K3 Superalloy in Cast State," (Proceedings on Cast Superalloy, Institute of Aeronautic Materials, Beijing, China, May 1982), 1-41.
5. Sun Chuanqi et al., "The Properties of DZ 3 Superalloy," Superalloys Handbook, (China, 1980), 940-947.
6. Sun Chuanqi et al., "A Study of the Castability of DZ3 DS Superalloy," Aeronautic Materials, 3(1984), 1-6.
7. J. H. Jackson et al., "The Effect of Volume Percent of Fine γ' on Creep in DS Mar-M200 + Hf," Met. Trans., 8A(10)(1977), 1615-1620.
8. Lin Dongliang (T. L. Lin), "Role of Solution Treatment in Improving the Creep Strength of a Directionally Solidified Nickel-Base Superalloy," Acta Metallurgica Sinica, 17(1)(1981), 26-37.
9. Lin Dongliang (T. L. Lin), Yao Deliang, Lin Xiangjin and Sun Chuanqi, "Effect of Volume Fraction and Size of Fine γ' on Creep Strength of a DS Nickel-Base Superalloy," Acta Metallurgica, 18(1)(1982), 104-114.
10. Lin Dongliang (T. L. Lin), Yao Deliang and Sun Chuanqi, "The Effect of Stress and Temperature on the Extent of Primary Creep in Directionally Solidified Nickel-Base Superalloys," Superalloys 1984, (M. Gell et al. eds., The Metallurgical Society of AIME), 187-200.
11. G. R. Leverat and D. N. Duhl, "The Effect of Stress and Temperature on the Extent of Primary Creep in Directionally Solidified Nickel-Base Superalloys," Met. Trans., 2(3)(1971), 907-908.